Nanoscale Horizons

Accepted Manuscript

ROYAL SOCIETY OF CHEMISTRY

rsc.li/nanoscale-horizons

Nanoscale Horizons

COMMUNICATION

Enhancing Single-Wall Carbon Nanotube Properties through Controlled Endohedral Filling

Received 00th January 20xx,
Accepted 00th January 20xx

DOI: 10.1039/x0xx00000x

www.rsc.org/

J. Campo,[a] Y. Piao,[b] S. Lam,[a] C. M. Stafford,[a] J. K. Streit,[a] J. R. Simpson,[b,c] A. R. H. Walker[b] and J. A. Fagan[a,†]

Chemical control of the endohedral volume of single-wall carbon nanotubes (SWCNTs) via liquid-phase filling is established to be a facile strategy to controllably modify properties of SWCNTs in manners significant for processing and proposed applications. Encapsulation of over 20 different compounds with distinct chemical structures, functionalities, and effects is demonstrated in SWCNTs of multiple diameter ranges, with the ability to fill the endohedral volume based on the availability of the core volume and compatibility of the molecule's size with the cross-section of the nanotube's cavity. Through exclusion of ingested water and selection of the endohedral chemical environment, significant improvements to the optical properties of dispersed SWCNTs such as narrowed optical transition linewidths and enhanced fluorescence intensities are observed. Examples of tailoring modified properties towards applications or improved processing by endohedral passivation are discussed.

Introduction

Spontaneous ingestion of solvent, typically water, during liquid-phase dispersion of single-wall carbon nanotubes (SWCNTs), and its deleterious effects on nanotube properties, is an endemic but often-neglected phenomenon with strong implications for the development of nanotube applications. Whether because of insufficient community awareness, view of these effects as higher order problems, or practical limitations due to the substantial additional effort required to isolate closed-ended (empty) SWCNTs after dispersion,[1,2] little literature work has focused on controlling the endohedral volume. This is despite observations such as narrower optical transition linewidths and significantly brighter fluorescence efficiencies (≈ 2.5X) for empty SWCNTs.[1] Water-filling furthermore modulates the exciton decay pathways,[3,4] and, given assignment of significant variance in device applications to exohedral water,[5,6] is potentially a significant source of trap states or other adverse effects for applications such as digital logic[7] or sensor platforms.[8,9]

In this contribution we demonstrate controlled filling of the SWCNT core with organic molecules of different structure and functionality through liquid-phase ingestion prior to aqueous or nonaqueous liquid-phase dispersion of the nanotubes. This novel capability leads to controllable modification (generally improvement) of SWCNT properties relative to uncontrolled solvent ingestion. Filling of immiscible, and to a lesser extent partially miscible, molecules, is found to be robust and applicable across multiple solvent systems. Our method is distinct from gas-phase (sublimation) –filling[10–17] in its ease and breadth, solution ingestion of salts or fullerenes in goals and scope,[18–23] and from previously investigated swelling of external micellar volumes on a dispersed nanotube's surface[24–27] in stability and flexibility. We also show, *vide infra*, that this filling is indeed solely endohedral in the dispersed SWCNT populations, and that those populations can readily be processed by literature SWCNT separation methods to obtain uniquely controlled sub-populations.

The primary motivation for this contribution is the idea of passivating the interior volume, *i.e.*, filling the nanotube with a low dielectric molecule to provide a barrier against water-filling while being generally non-disruptive to the electronic structure of the SWCNT. This does not imply that more active molecules cannot be encapsulated through liquid phase ingestion, as recently demonstrated for purposes beyond serving as a passive modifying agent.[28,29] The size of the endohedral volume to be filled depends on the specific structure of each nanotube species (chirality), defined by the vector pair (*n,m*) which describes the wrapping vector of the hexagonal carbon lattice comprising the cylindrical nanotube.[30] Depending on the (*n,m*) species, and assuming an exclusion distance from the carbon lattice similar to the interlayer spacing in graphite, ≈ 0.34 nm, the diameter of the circular

[a] *National Institute of Standards and Technology, Materials Science and Engineering Division, Gaithersburg, MD USA 20899.*
[b] *National Institute of Standards and Technology, Engineering Physics Division, Gaithersburg, MD USA 20899.*
[c] *Towson University, Department of Physics, Astronomy, and Geosciences, Towson, MD 21252*
† Corresponding Author: jeffrey.fagan@nist.gov

Electronic Supplementary Information (ESI) available: additional experimental details, demonstrations of filling with alternate cyclic and linear compounds, further optical characterization of filled SWCNTs, example photographs of the purification process and alternate experiments supporting the ingestion of the filler molecules. See DOI: 10.1039/x0xx00000x

core cross-section varies from < 0.5 nm to > 2 nm across commercially available SWCNT populations. Importantly, water is known to fill even the smallest diameter nanotubes,[31] whereas it can be expected that filling molecules larger than water should exhibit a size-dependent sieving threshold, as indeed demonstrated for a stilbene-based molecule.[29] As an initial set of test molecules, saturated linear and cycloalkanes are obvious choices for examining the effects of passivation along with the size-dependent effects of endohedral filling.

Results and discussion

Absorbance spectra of electric arc (EA) SWCNTs, average diameter ≈ 1.45 nm, dispersed in aqueous sodium deoxycholate (DOC) solution with six different endohedral fillings besides/in addition to water are shown in Fig. 1a. Peak features in the spectra arise from the strong interband optical transitions of each SWCNT species, with the groupings of transitions related to the S_{11} (1400 to 2000) nm, S_{22} (≈ 850 to 1200) nm, M_{11} (≈ 600 to 800) nm, S_{33} (≈ 450 to 550) nm and higher order transitions; S_{ii} and M_{ii} indicate the interband optical transitions for semiconducting and metallic nanotube species, respectively. An important primary observation is that the wavelength of each peak feature is significantly different across the spectra in Fig. 1a with three groupings: empty nanotubes display sharp, blue-shifted, peak positions; water-filled nanotubes broad, red-shifted, peak positions, and alkane-filled nanotubes sharp peaks with wavelengths closer to the empty than water-filled positions. Spectra for SWCNT populations encapsulating linear alkanes of other lengths as well as 16 additional linear and cyclic alkane variants are shown in the Electronic Supplementary Information (ESI).

Prior contributions have recognized the environmental dependence of the optical transition energies of the SWCNTs in terms of a solvatochromic effect sensitively influenced by the surrounding (encapsulated) dielectric environment.[3,21,25,26,32–35] However, effects from interior and exterior environments are infrequently distinguished. In the data presented in Fig. 1, the external environment is common to each of the dispersions, and thus the observed peak shifts are direct evidence of successful filling with the specified alkane compounds for these larger diameter nanotubes (average carbon centers definition diameters of ≈ 1.45 nm). For each of the shown encapsulation examples, ingestion was accomplished simply through immersion of the dry parent soot in a volume of the liquid material (see section S1 in the ESI for experimental details). Endohedral filling is spontaneous and likely occurs rapidly, although we exposed each soot for ≈ 24 h. Exohedral molecules are removed through filtration of the soot from the bulk liquid, followed by a rinse step with a solvent for the filling molecule, typically ethyl acetate. Likely due to steric effects from the SWCNTs already being filled, this solvent is not encapsulated. Dispersion of the nanotubes is then performed using the filled-core SWCNTs as the parent material in typical aqueous or non-aqueous dispersion procedures. Importantly, qualitatively little change, possibly even improvement, is observed in the dispersion efficiency (for well-rinsed powders) on a mass basis (ESI), while the optical properties of the achieved SWCNT dispersion are dramatically improved.

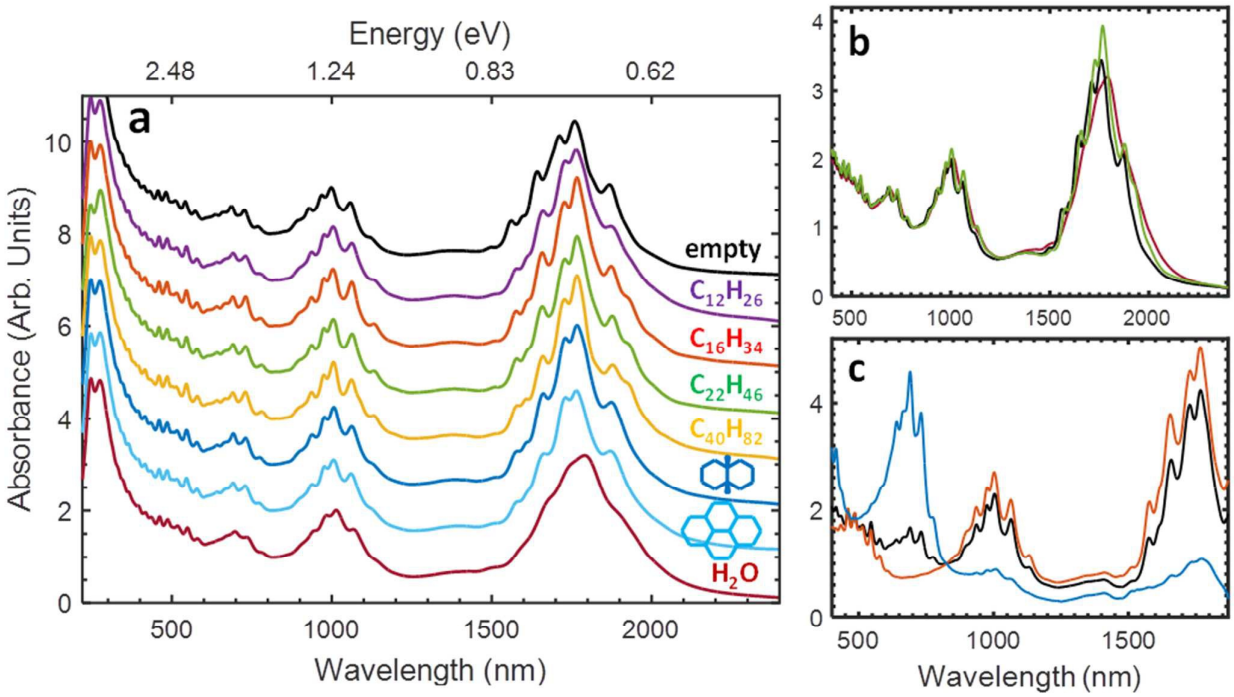

Fig. 1 (a) Absorbance spectra of EA SWCNTs dispersed in aqueous sodium deoxycholate (DOC) solutions with different endohedral fillings (vertical offset 1 unit/spectra). From top: empty core, dodecane-filled, hexadecane-filled, docosane-filled, tetracontane-filled, *cis*-decalin-filled, perhydropyrene-filled, and water-filled. The optical transition peaks exhibited by the alkane-filled nanotubes are similar to each other, while intermediate in position and breadth to the empty and water-filled nanotubes. (b) Absorbance spectra of empty (black), docosane-filled (green) and water-filled (red) nanotubes from panel (a), without vertical offset. Narrower optical transition linewidths concentrate the optical intensity of the SWCNT peak features. (c) Absorbance spectra of aqueous two-phase extraction isolated metallic (blue) and semiconducting (red) SWCNT populations of octadecane-filled SWCNTs (black). All spectra are normalized at their 810 nm valley.

Qualitatively, the sharpness (*i.e.,* reduced apparent peak width) of the alkane-filled peak features in Fig. 1a generally improves with increasing alkane chain length, with a different distribution structure observed for cyclic filler molecules. These populations were all purified in the same manner, and thus this variation probably reflects molecular packing differences, such as molten *vs.* solidified core volumes, more so than purity differences across the shown samples. To further highlight this, Fig. 1b presents the spectra of the empty, docosane ($C_{22}H_{46}$)-filled, and water-filled EA SWCNTs from Fig. 1a without the offset. Plotted in this manner, the narrower transition linewidths and blue-shifted peak positions of the empty and docosane-filled SWCNTs compared to the water-filled SWCNTs are clearly apparent, as is the equivalence of the diameter distribution (common range of absorbance transitions) in the three samples. Lastly, since only D_2O/DOC contributions to the absorbance are subtracted in the shown spectra, the similarity in the total integrated intensity of the three spectra indicate equivalent cleanliness of the populations being compared, and that the filling process does not result in additional impurities being dispersed.

Large-scale utility of controlling the endohedral environment is only truly useful if it can be accomplished without disrupting the applicability of other processing methodologies for separating subpopulations of nanotubes. Fig. 1c shows the absorbance spectra of separated metallic and semiconducting populations of hexadecane-filled SWCNTs generated *via* aqueous two-phase extraction (ATPE) without modification to the reported procedure.[36,37] Separation of the two sub-populations is hence consistent with the previous separations of water-filled or empty SWCNTs, and the peak positions associated with endohedral filling are unchanged by the separation. This demonstrates that the alkane-filling is robust to the separation procedure and *vice versa*. Endohedral filling can furthermore be easily applied to improve nanotube separations such as density gradient ultracentrifugation (DGU)[38] by utilizing a significantly denser (lighter) than water filler molecule such as a halogenated alkane (linear alkane) to increase (decrease) the spread in buoyant densities (ESI).

The observation that all 22 liquefiable neat organic molecules tested were encapsulated *via* the simple filling procedure implies that each of the molecules can adopt a conformation(s) fitting within the available cavities of the EA SWCNTs. SWCNTs of the cobalt-molybdenum catalyst (CoMoCat)[39] or high pressure CO disproportionation (HiPco) methods, however, are significantly smaller in diameter and thus are likely to display size-dependent encapsulation. In Fig. 2, absorbance spectra are shown for CoMoCat and HiPco SWCNT populations without controlled filling (water-filled), exposed to hexadecane pre-dispersion, and exposed to *cis*-decalin pre-dispersion. Clear shifts indicative of endohedral filling by the linear alkane are apparent for almost all optical transition peak positions for the hexadecane-exposed nanotubes relative to their water-filled controls. Although the (7,5) S_{11} peak (at 1033 nm) and several others are not observed to shift, S_{11} features originating from the significantly smaller diameter (6,5) and (9,1) SWCNT species do shift,

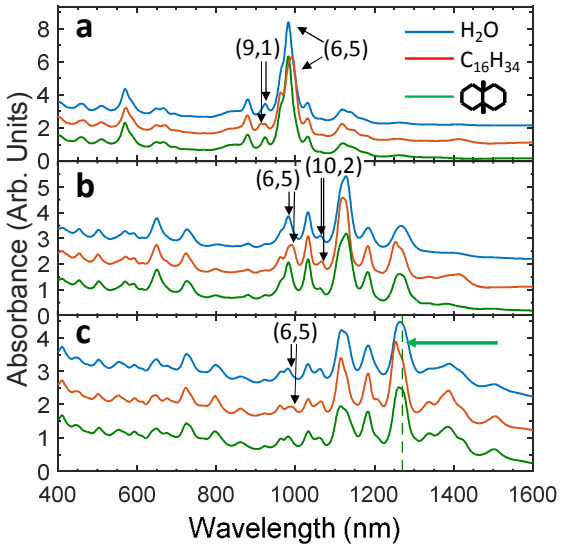

Fig. 2 (a) Absorbance spectra of small diameter (< ≈ 1.15 nm) SWCNTs after purification from (a) CoMoCat SG65i, (b) CoMoCat EG150, and (c) HiPco synthesis methods without controlled filling (blue, water-filled), exposed to hexadecane pre-dispersion (red), and exposed to cis-decalin pre-dispersion (green). The dashed line and green arrow indicate the apparent threshold filling diameter for cis-decalin. To aid comparison, spectra were scaled to equal one at the valley between the S11 and S22 transitions and then vertically offset by 1 unit. Black arrows in each group of spectra highlight the absorbance peak shifts of the (9,1), (6,5) and (10,2) species, demonstrating that alkane filling is present in these nanotubes. An expanded view of the S11 region is provided in the ESI.

indicating it is likely that all SWCNT species > 0.757 nm diameter can fill with the linear alkane. The lack of clear peak shifts in absorbance for SWCNT species having a diameter above this threshold thus may indicate that either they are not filling due to structure-specific packing effects, or that the specifics of the filling affect the optical transitions in a manner more complicated than simple dielectric modulation in the small diameter SWCNT limit. The latter hypothesis is supported by the observation that the S_{11} peaks for the equal diameter (6,5) and (9,1) SWCNT species shift in opposite directions (red *versus* blue shifted respectively) with alkane filling; fluorescence and Raman scattering results (*vide infra)* are also consistent with this view. Interestingly, the opposite shifts of the (6,5) and (9,1) SWCNT species are made more obvious because not all of these SWCNTs are being filled with exposure to the alkane. We hypothesize that this is likely due to partially blocked access to the nanotube interior during the filling process, as prior results for water-filling indicate that SWCNTs either fill completely or not at all.[3] In fact, for the small diameter nanotubes, we found that additional processing (furnace annealing, see ESI) was necessary to enable filling during alkane exposure even when the parent soot would spontaneously fill with water. Once annealed however, bimodal features in optical characterization are not observed for SWCNTs larger in diameter than the (6,5) tube (*vide infra*), which suggests that the fraction filled by the hexadecane must approach 100%. Partial filling of the (6,5) tube may thus be an artefact of our non-optimized annealing methodology.

In contrast to the hexadecane results, and the results for EA SWCNTs, the significantly wider cyclic molecule *cis*-decalin is not uniformly encapsulated in the small diameter SWCNT

populations. As would be expected for size sieving-based exclusion, none of the peaks in the absorbance spectra for the CoMoCat SG65i or EG150 materials visibly shift from their water-filled positions with attempted *cis*-decalin filling. In the somewhat larger average diameter HiPco SWCNT population, only S_{11} absorbance features > 1310 nm are affected significantly by *cis*-decalin exposure (*i.e.*, peaks due to SWCNTs larger than those found in the EG150 population). These observations imply a threshold size for filling of approximately the (9,7) chirality diameter (1.103 nm), matching a previous sieving threshold observed by Cambré *et al.*[29] for filling SWCNTs with a similar, but conjugated and therefore more rigid, ring structure dye molecule *p,p'*-dimethylaminonitrostilbene. More sensitive fluorescence-excitation and Raman measurements on the *cis*-decalin treated EG150 sample (*vide infra*) modify this observation somewhat and imply that the threshold is instead the slightly smaller (8,6) SWCNT species, which is not well resolved in the absorbance data due to spectral congestion. Also of note is that the presence or absence of peak shifts for each of the common SWCNT chiralities is consistent regardless of the parent material, illustrating both the reproducibility and consistency of the applied filling procedure.

The observation that attempted filling of small diameter nanotubes with larger molecules yields water-filled SWCNT spectra not only implies the expected presence of a sieving phenomenon in the filling process, but also provides evidence that the observed spectral shifts are not due to alternative explanations such as exterior adsorption or cleaning of the nanotube surfaces *via* the pre-dispersion exposure to the organic molecule. Additional experiments (ESI) also show that the effect observed here is very different from the effect of transient micelle swelling observed previously[26] for SDS-coated SWCNTs in aqueous dispersions in which various hydrophobic solvents were added and then allowed to evaporate. Briefly, water-filled SWCNTs in DOC/water show no spectral changes after mixing with an alkane solvent (ESI), nor do alkane/cycloalkane-filled SWCNTs change their spectral positions even if the dispersion DOC/H_2O medium is exchanged for DOC/D_2O *via* multiple ultrafiltration/dilution steps. These results are consistent with endohedral filling rather than a micelle swelling phenomenon. Moreover, closed-ended and therefore empty SWCNTs are found to be unaffected by exposure to alkanes (ESI).

We also performed polarization-modulation infrared reflection-absorption spectroscopy (PM-IRRAS), X-ray photoelectron spectroscopy (XPS), analytical ultracentrifugation (AUC), fluorescence-excitation spectroscopy and Raman spectroscopy to validate the endohedral filling. For PM-IRRAS and XPS measurements, perfluorooctane (C_8F_{18})@EA SWCNTs and water-filled EA SWCNT dispersions were filtered and extensively washed to produce a pair of nominally surfactant-free nanotube buckypapers for the measurement. In both experiments, only the exposed film expected to contain endohedral perfluorooctane displays features associated with the presence of fluorine, with particularly clear observation of a significant quantity of fluorine in the XPS spectra (ESI). As both buckypapers were processed identically, extensively washed, and exposed to high vacuum, the presence of fluorine in only the exposed sample film is a strong indicator that perfluorooctane was ingested as proposed.

Similarly, density contrast measurements on different dispersed alkane-filled SWCNT populations in the AUC[40,41] resulted in findings consistent only with the filling of the endohedral cavity by the expected molecule. Previously, we measured an average anhydrous density of (1317 $\pm$ 10) kg/m^3 for empty EA SWCNT, and $\approx$ 1530 kg/m^3 for water-filled EA SWCNT.[42] Based on these values and the bulk densities of water, the applied linear alkane ($C_{22}H_{46}$), and C_8F_{18} (1000 kg/m^3, 778 kg/m^3 and 1777 kg/m^3 respectively), expected values of 1483 kg/m^3 and 1692 kg/m^3 for $C_{22}H_{46}$ and C_8F_{18} filled SWCNTs can be projected, respectively, if the filling efficiency is similar for the three materials. Our actual measured values for the water, $C_{22}H_{46}$, and C_8F_{18} filled populations, shown in Fig. S10 (ESI), are (1510 $\pm$ 19) kg/m^3, (1429 $\pm$ 13) kg/m^3, and (1564 $\pm$ 17) kg/m^3 respectively. These data are consistent with the expected relative filler densities, but indicative that the bulkier tetracosane and perfluorooctane molecules each pack at a reduced molecular density relative to water (a much smaller molecule) and their unconstrained bulk densities ($\approx$ 75 % and 71 % respectively).

Lastly, the frequencies of the resonant radial breathing modes (RBMs) in Raman scattering were measured for small diameter CoMoCat and HiPco SWCNTs (Fig. 3) and large diameter EA SWCNTs (Figs S10 and S11) of both alkane and water-filled populations at selected excitation wavelengths. In each case, clear shifts of the RBM frequencies were observed for most of the probed species. Note that Raman RBM modes are only observed for SWCNTs for which the excitation laser energy is sufficiently close in energy to their optical transitions.[43] Interestingly, both hardening (*i.e.*, shifts towards higher frequency, indicating greater phonon energy of the vibration) and softening (*i.e.*, shifts towards lower frequency) of the RBM frequencies were observed for the alkane-filled tubes relative to the water-filled RBM frequencies of the different species of SWCNTs. This is likely caused by different

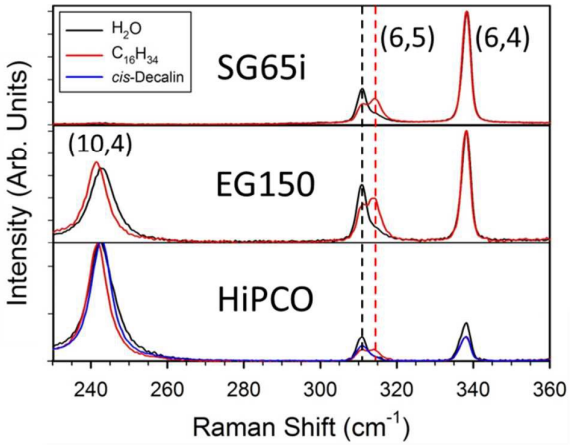

arrangements of the ingested alkane inside the core volume of the various diameter SWCNTs, as has also been observed for

Fig. 3 Resonant Raman spectra from 575 nm excitation of small diameter SWCNTs after purification from (a) CoMoCat SG65i, (b) CoMoCat EG150, or (c) HiPco synthesis methods without controlled filling (black, water-filled), exposed to hexadecane pre-dispersion (red), or exposed to cis-decalin pre-dispersion (blue). Upon hexadecane filling, the RBM of the (6,5) SWCNT at $\approx$ 314 cm^{-1} is found to harden compared to water-filling, whereas the RBM of the (10,4) SWCNT at $\approx$ 241 cm^{-1} is softened. For the (6,4) SWCNT on the other hand, no shift is observed, likely indicating that this tube is not filling with either alkane subjected to the applied processing conditions.

some gas-phase filled molecules.[44] The observed RBMs with filling are, however, always hardened compared to those for empty nanotubes.[31,45] It is clear from Fig. 3 that only part of the RBM intensity of the alkane-exposed (6,5) species hardens relative to the reference water-filled sample, indicating that only a part of the (6,5) population is alkane-filled with the utilized processing. That the hardened shoulder originates from the hexadecane-filled fraction is confirmed by the Raman resonance energy profile (ESI). The RBM of the (7,5) species is also measurably hardened relative to water-filling (≈ 0.7 cm^{-1}, Fig. S12), indicating that the lack of an absorbance peak shift is likely due to structural packing effects of the alkane rather than a lack of filling. Lastly, the (6,4) SWCNT is unchanged in spectral position in both absorbance and Raman RBM measurements, suggesting that the linear alkane is not ingested in this SWCNT under the applied processing, although it is also possible that the alkane-filling simply yields undistinguishably changed values.

In addition to the effects on the absorbance and RBM peak positions, it is also anticipatable on the basis of comparison to empty *vs.* water-filled nanotube optical properties[1–3] that the near-infrared (NIR) fluorescence of alkane-filled SWCNTs should be significantly enhanced relative to water-filled populations. A comparison of excitation-emission contour plots for the small-diameter EG150 CoMoCat populations with hexadecane and water-filling, shown in Fig. 4, immediately validates this hypothesis. Emission intensity is indeed

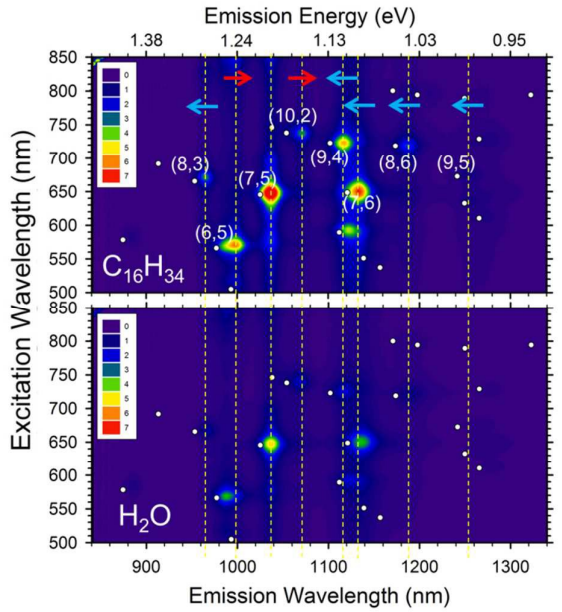

significantly increased for hexadecane-filling, with comparison of intensities for the most prominent species yielding ratios of ≈ 2.5 X to 3 X at the peak positions for the alkane-filled SWCNTs; the exception is the (6,4) SWCNT, which is unchanged within measurement uncertainty, consistent with the above indications that it is not filled by the linear alkane. These enhancements in fluorescence intensity are similar to those observed for empty SWCNTs (≈ 2.5 X)[3] relative to water-filled SWCNTs. Additional experiments with laser excitation, time or single particle resolution, purified populations and integration of emission intensity will be required to establish exact values and sources for the improvement.

Fig. 4 Excitation-emission contour plots of hexadecane-filled (top) and water-filled (bottom) EG150 CoMoCat SWCNTs. Both samples were measured at the same concentration (as determined by absorbance) and under identical conditions. The alkane-filled sample exhibits a notable increase in fluorescence intensity, along with shifts in emission and excitation wavelengths consistent with those measured in absorbance. To aid in comparison, vertical dashed lines are shown that pass through the peak positions observed for select alkane-filled (*n*,*m*) species; the red or blue arrows further indicate the direction of the peak shift relative to the observed water-filled peak. White dots, indicating fluorescence peak locations for small diameter (n,m) species dispersed in SDS, are shown for comparison.[57]

Focusing on the different chiralities, consistent peak shifts are observed in the absorbance and fluorescence measurements (both in emission and excitation). Notably, however, although the fluorescence peak of the (7,5) SWCNT does not show a shift with alkane filling (as in the absorbance spectra), the intensity is increased relative to the water-filled SWCNTs; this indicates, along with the RBM shift (Fig. 3), that this species is indeed alkane filled.

Literature reports describing shifts of SWCNT transitions in various (exohedral) environments *vs.* SWCNTs in vacuum or air explain this behavior in the context of solvatochromism, which is the reduction in energy of the optical transitions due to the stabilization of the excited state by the dielectric medium (solvent Stark effect).[25,32–35,46] Here, we have the opportunity to look at the shifts induced by endohedral filling. Comparing the peak positions of hexadecane-filled SWCNTs and water-filled SWCNTs in either Fig. 1 or Fig. 3, to those reported for empty SWCNTs in DOC/D_2O,[1,3] we find that alkane-filling redshifts all SWCNT transitions relative to vacuum, but generally significantly less than water-filling induces. These behaviors are expected based on each alkane's lesser, but still greater than vacuum/air, dielectric constant relative to water's dielectric constant. Additionally, the endohedral alkane-filling driven shifts (ranging from less than -1 meV up to more than -15 meV) are generally smaller than exohedral-driven shifts reported for SWCNTs in apolar microenvironments.[25] From an engineering standpoint, control of the dielectric constant should enable choice of smaller shifts by filling with low dielectric compounds and larger shifts from high dielectric compounds, although the actual shifts will also be affected by specific molecule-SWCNT chemical, physical or higher order electronic interactions.

For more advanced analysis of the solvatochromic description of these effects we examine the endohedral-filling driven shifts *vs.* SWCNT diameter (by plotting $E_{11}^3 \cdot \Delta E_{11}$ *vs.* $1/d^5$ as in Silvera-Batista *et al.*[25] and Larsen *et al.*,[35] Fig. 5), revealing an increasing effect with decreasing diameter for both alkane-filling and water filling. This is similar, but smaller in magnitude, to the behavior reported in exohedral apolar solvents.[25] However, while exohedral shifts are reported to closely follow a linear behavior, the endohedral shifts observed here display, especially for the alkane-filling, clear chirality-dependent variation from the average trend. Most likely, the narrower SWCNTs especially, are sensitive to the particular arrangement of the encapsulated alkane, which will in turn depend on the exact geometry of the different SWCNT. Indeed, even SWCNTs of different species but identical diameter can exhibit markedly different spectral shifts (*e.g.*, the (6,5) and (9,1) SWCNTs show respective shifts of ≈ -15 meV

and -4 meV). These results are not surprising given the geometric differences between internal filling and external surrounding[47,48] and the packing variations likely to be encountered due to the near-atomic length scale of the pore cross sections.[13]

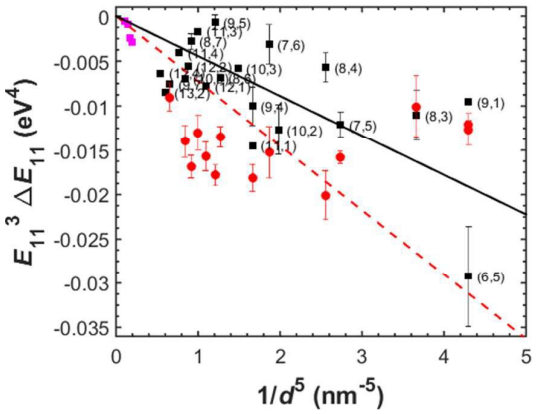

Fig. 5 Solvatochromic shift values for the lowest-energy transitions (E_{11}) of water-filled SWCNTs (red circles), hexadecane-filled EA SWCNTs (magenta squares) and hexadecane-filled narrow diameter SWCNTs (average position from SG65i, EG150 and HiPco populations; black squares) relative to empty SWCNTs in D_2O ($\Delta E_{11} = E_{11}^{filled} - E_{11}^{empty}$, d = SWCNT diameter). Lines are linear fits to the data (hexadecane = solid black line, water = red dashes). Due to the smaller dielectric constant of the hexadecane, the magnitude of the linear fit slope is much reduced compared to water-filling. Both data sets, however, display significantly greater scatter about the linear trend then reported for exohedral environmental changes. Values for the EA SWCNTs are estimated from the absorption spectra of the hexadecane-filled and empty samples using an average diameter values for each peak reflecting the multiple SWCNT species most likely contributing to that feature. Values for the narrow diameter SWCNTs are obtained from measured fluorescence peak positions. Peak positions for purely empty SWCNTs in DOC/D2O and water-filled SWCNTs in DOC/D2O are from references [1] and [3]. Error bars on hexadecane-filled points represent the variation in peak positions measured from the different SWCNT parent soot materials. As all soot materials were processed identically, this variation is likely due to diverse pre-treatments by the manufacturers influencing the degree of alkane-filling; this would result in some peak positions reflecting convoluted water-filled and alkane-filled peak values rather than the purely alkane-filled value.

A common feature of nearly all of the compounds presented for encapsulation is their relative to near total immiscibility with the bulk solvent (water). As it is also possible to disperse nanotubes in non-aqueous environments, it is worth noting that extemporaneous solvent-filling is almost certainly present in those circumstances, and should also be subject to exclusion by intentional pre-encapsulation of an immiscible compound. A comparison of poly[(9,9-dioctylfluorenyl-2,7-diyl)-alt-co-(6,60-{2,20-bipyridine})] (PFO-BPY) dispersed SWCNTs in toluene[49] with/without encapsulation of perfluorooctane (C_8F_{18}) is shown in the ESI to demonstrate the broad applicability of the phenomenon. Interestingly, we also have evidence for stable encapsulation (over months) of volatile and/or even water-miscible solvents in SWCNTs dispersed in water/DOC, including pentane and ethyl acetate (ESI). A possible explanation for this observation is that the DOC dispersant molecules may "cap the bottle" on the endohedral contents given the processing method, which would further broaden the utility of incorporating controlled filling.

Optical linewidth improvements are not the sole justification for incorporating an endohedral filling molecule into a SWCNT. Ingestion of cations along with water during dispersion with ionic surfactants may be a particularly pernicious, and to date unexamined, source of nanotube device variation made from solution-separated materials. Passivation of the core volume with a passive hydrocarbon should prevent such ingestion[50] while still being removable by typical heating/vacuum processes used in device fabrication. Similarly, the increase in fluorescence intensity of narrow-band emitting, small diameter SWCNT populations by alkane-filling will improve the potential for effective SWCNT-based sensors, devices, and theragnostic applications,[51] given that empty nanotubes are difficult to isolate and are only present, if at all, in small fractional percentage, < 10 %, in most SWCNT materials. Alkane-filling instead offers a near 100 % efficient redirection of would be water-filled into alkane-filled SWCNTs enabling the use of tailored optical properties and reduced material variation through a simple, high-yield process. We lastly point out that simple controlled endohedral filling enables a broad swath of previously non-performable scientific investigations. Empowered investigation directions will include measurements of molecular self-diffusion and melting/boiling point effects in highly constrained one-dimensional cavities (of selectable diameter),[52,53] attempts at contrast improvements for scattering techniques, as well as application of modified nanotube properties for optimization of other separations strategies such as DGU. Straight forward expansion of the method to include ingestion of active molecules points furthermore towards, doping control, investigation of SWCNT deformation by confined molecules,[23,54] directionally constrained polymerization,[55] and/or controlled endohedral chemical modification of the nanotube sp^2 lattice.[56]

Conclusions

Effective and controllable filling of SWCNTs with a wide range of organic compounds through liquid-phase exposure prior to nanotube dispersion is demonstrated, with stable encapsulation achieved for all cases in which the compound is both small enough to fit into the SWCNT and sufficiently immiscible with the post-dispersion bulk liquid environment. For alkane and alkane derivatives, encapsulation is further shown to enable tunable modulation of optical and other physical properties of the combined SWCNT/guest molecule complex such as density. These results have positive implications for technologies based on well-resolved optical properties, modulated separations, or which are sensitive to increased variation in properties caused by filling. It is expected that this report will enable a large number of additional studies relating to phase transitions and transport in highly confined geometries.

Acknowledgements

S.L. and J.S. gratefully acknowledge support of National Research Council Postdoctoral Fellowships.

Notes and references

1 S. Cambré and W. Wenseleers, *Angew. Chemie - Int. Ed.*, 2011, **50**, 2764–2768.
2 J. A. Fagan, J. Y. Huh, J. R. Simpson, J. L. Blackburn, J. M.

Holt, B. A. Larsen and A. R. H. Walker, *ACS Nano*, 2011, **5**, 3943–3953.
3 S. Cambré, S. M. Santos, W. Wenseleers, A. R. T. Nugraha, R. Saito, L. Cognet, B. Lounis, S. Cambre, S. M. Santos, W. Wenseleers, A. R. T. Nugraha, R. Saito, L. Cognet and B. Lounis, *ACS Nano*, 2012, **6**, 2649–2655.
4 J. G. Duque, L. Oudjedi, J. J. Crochet, S. Tretiak, B. Lounis, S. K. Doorn and L. Cognet, *J. Am. Chem. Soc.*, 2013, **135**, 3379–3382.
5 Q. Qian, G. Li, Y. Jin, J. Liu, Y. Zou, K. Jiang, S. Fan and Q. Li, *ACS Nano*, 2014, **8**, 9597–9605.
6 T. J. Ha, D. Kiriya, K. Chen and A. Javey, *ACS Appl. Mater. Interfaces*, 2014, **6**, 8441–8446.
7 G. S. Tulevski, A. D. Franklin, D. Frank, J. M. Lobez, Q. Cao, H. Park, A. Afzali, S. J. Han, J. B. Hannon and W. Haensch, *ACS Nano*, 2014, 8, 8730–8745.
8 F. Michelis, L. Bodelot, Y. Bonnassieux and B. Lebental, *Carbon N. Y.*, 2015, **95**, 1020–1026.
9 B. Y. Lee, M. G. Sung, J. Lee, K. Y. Baik, Y. K. Kwon, M. S. Lee and S. Hong, *ACS Nano*, 2011, **5**, 4373–4379.
10 H. Kataura, Y. Maniwa, T. Kodama, K. Kikuchi, K. Hirahara, K. Suenaga, S. Iijima, S. Suzuki, Y. Achiba and W. Krätschmer, *Synth. Met.*, 2001, **121**, 1195–1196.
11 D. A. Morgan, J. Sloan and M. L. H. Green, *Chem. Commun.*, 2002, 2442–3.
12 T. Takenobu, T. Takano, M. Shiraishi, Y. Murakami, M. Ata, H. Kataura, Y. Achiba and Y. Iwasa, *Nat. Mater.*, 2003, **2**, 683–8.
13 J. Lu, S. Nagase, D. Yu, H. Ye, R. Han, Z. Gao, S. Zhang and L. Peng, *Phys. Rev. Lett.*, 2004, **93**, 9–12.
14 K. Yanagi, Y. Miyata and H. Kataura, *Adv. Mater.*, 2006, **18**, 437–441.
15 D. Nishide, H. Dohi, T. Wakabayashi, E. Nishibori, S. Aoyagi, M. Ishida, S. Kikuchi, R. Kitaura, T. Sugai, M. Sakata and H. Shinohara, *Chem. Phys. Lett.*, 2006, **428**, 356–360.
16 M. A. Loi, J. Gao, F. Cordella, P. Blondeau, E. Menna, B. Bartova, C. Hebert, S. Lazar, G. A. Botton, M. Milko and C. Ambrosch-Draxl, *Adv. Mater.*, 2010, **22**, 1635–1639.
17 T. Fujimori, A. Morelos-Gómez, Z. Zhu, H. Muramatsu, R. Futamura, K. Urita, M. Terrones, T. Hayashi, M. Endo, S. Young Hong, Y. Chul Choi, D. Tománek and K. Kaneko, *Nat. Commun.*, 2013, **4**, 2162.
18 J. Sloan, J. Hammer, M. Zwiefka-Sibley, M. L. H. Green and J. Sloan, *Chem. Commun.*, 1998, 347–348.
19 F. Simon, H. Kuzmany, H. Rauf, T. Pichler, J. Bernardi, H. Peterlik, L. Korecz, F. Fülöp and A. Jánossy, *Chem. Phys. Lett.*, 2004, **383**, 362–367.
20 F. Simon, H. Kuzmany, J. Bernardi, F. Hauke and A. Hirsch, *Carbon N. Y.*, 2006, **44**, 1958–1962.
21 S. Okubo, T. Okazaki, K. Hirose-Takai, K. Suenaga, S. Okada, S. Bandow and S. Iijima, *J. Am. Chem. Soc.*, 2010, **132**, 15252–15258.
22 M. Vizuete, M. Barrejón, M. J. Gómez-Escalonilla and F. Langa, *Nanoscale*, 2012, **4**, 4370–81.
23 A. N. Khlobystov, *ACS Nano*, 2011, 5, 9306–9312.
24 C. A. Silvera-Batista and K. J. Ziegler, *Langmuir*, 2011, **27**, 11372–11380.
25 C. a Silvera-Batista, R. K. Wang, P. Weinberg and K. J. Ziegler, *Phys. Chem. Chem. Phys.*, 2010, **12**, 6990–6998.
26 R. K. Wang, W. C. Chen, D. K. Campos and K. J. Ziegler, *J. Am. Chem. Soc.*, 2008, **130**, 16330–16337.
27 C. Roquelet, J.-S. Lauret, V. Alain-Rizzo, C. Voisin, R. Fleurier, M. Delarue, D. Garrot, A. Loiseau, P. Roussignol, J. A. Delaire and E. Deleporte, *Chemphyschem*, 2010, **11**, 1667–72.
28 E. Gaufrès, N. Y.-W. Tang, F. Lapointe, J. Cabana, M.-A. Nadon, N. Cottenye, F. Raymond, T. Szkopek and R. Martel, *Nat. Photonics*, 2013, **8**, 72–78.
29 S. Cambré, J. Campo, C. Beirnaert, C. Verlackt, P. Cool and W. Wenseleers, *Nat. Nanotechnol.*, 2015, **10**, 248–52.
30 M. S. Dresselhaus and P. Avouris, in *Carbon Nanotubes: Synthesis, Structure, Properties, and Applications*, eds. M. S. Dresselhaus, G. Dresselhaus and P. Avouris, Springer: Berlin, 2001, pp. 1–9.
31 S. Cambré, B. Schoeters, S. Luyckx, E. Goovaerts, W. Wenseleers, S. Cambr??, B. Schoeters, S. Luyckx, E. Goovaerts and W. Wenseleers, *Phys. Rev. Lett.*, 2010, **104**, 1–4.
32 Y. Ohno, S. Iwasaki, Y. Murakami, S. Kishimoto, S. Maruyama and T. Mizutani, in *Physica Status Solidi (B) Basic Research*, 2007, vol. 244, pp. 4002–4005.
33 J. H. Choi and M. S. Strano, *Appl. Phys. Lett.*, 2007, **90**, 14–17.
34 J. Gao, W. Gomulya and M. A. Loi, *Chem. Phys.*, 2013, **413**, 35–38.
35 B. A. Larsen, P. Deria, J. M. Holt, I. N. Stanton, M. J. Heben, M. J. Therien and J. L. Blackburn, *J. Am. Chem. Soc.*, 2012, **134**, 12485–12491.
36 C. Y. Khripin, J. A. Fagan and M. Zheng, *J. Am. Chem. Soc.*, 2013, **135**, 6822–6825.
37 H. Gui, J. K. Streit, J. A. Fagan, A. R. Hight Walker, C. Zhou and M. Zheng, *Nano Lett.*, 2015, **15**, 1642–1646.
38 M. S. Arnold, A. A. Green, J. F. Hulvat, S. I. Stupp and M. C. Hersam, *Nat. Nanotechnol.*, 2006, **1**, 60–65.
39 *Certain equipment, instruments or materials are identified in this paper in order to adequately specify the experimental details. Such identification does not imply recommendation by the National Institute of Standards and Technology (NIST) nor does it im*, .
40 P. H. Brown, A. Balbo, H. Zhao, C. Ebel and P. Schuck, *PLoS One*, 2011, **6**.
41 J. A. Fagan, M. Zheng, V. Rastogi, J. R. Simpson, C. Y. Khripin, C. A. Silvera Batista and A. R. Hight Walker, *ACS Nano*, 2013, **7**, 3373–3387.
42 C. A. Silvera Batista, M. Zheng, C. Y. Khripin, X. Tu and J. A. Fagan, *Langmuir*, 2014, **30**, 4895–904.
43 J. Maultzsch, H. Telg, S. Reich and C. Thomsen, *Phys. Rev. B - Condens. Matter Mater. Phys.*, 2005, **72**.
44 Y. Almadori, L. Alvarez, R. Le Parc, R. Aznar, F. Fossard, A. Loiseau, B. Jousselme, S. Campidelli, P. Hermet, A. Belhboub, A. Rahmani and T. Saito, 2014.
45 M. J. Longhurst and N. Quirke, *J. Chem. Phys.*, 2006, **125**.
46 A. R. T. Nugraha, R. Saito, K. Sato, P. T. Araujo, A. Jorio and M. S. Dresselhaus, *Appl. Phys. Lett.*, 2010, **97**.

47 T. Ando, in *Physica E: Low-Dimensional Systems and Nanostructures*, 2011, vol. 43, pp. 798–803.
48 S. Uryu and T. Ando, *Phys. Rev. B - Condens. Matter Mater. Phys.*, 2012, **86**, 125412.
49 K. S. Mistry, B. A. Larsen and J. L. Blackburn, *ACS Nano*, 2013, **7**, 2231–2239.
50 O. Byl, J. Liu and J. T. Yates, *Carbon N. Y.*, 2006, **44**, 2039–2044.
51 D. Roxbury, P. V. Jena, Y. Shamay, C. P. Horoszko and D. A. Heller, *ACS Nano*, 2015, acsnano.5b05438.
52 J. Jiang and S. I. Sandler, *Langmuir*, 2006, **22**, 7391–7399.
53 S. Shimizu, K. V. Agrawal, M. O'Mahony, L. W. Drahushuk, N. Manohar, A. S. Myerson and M. S. Strano, *Langmuir*, 2015, **31**, 10113–10118.
54 J. H. Warner and M. Wilson, *ACS Nano*, 2010, **4**, 4011–4016.
55 J. Steinmetz, S. Kwon, H. Lee, E. Abou-hamad, R. Almairac, C. Goze-bac, H. Kim and Y. Park, *Chem. Phys. Lett.*, 2006, **431**, 139–144.
56 Y. Piao, B. Meany, L. R. Powell, N. Valley, H. Kwon, G. C. Schatz and Y. Wang, *Nat. Chem.*, 2013, **5**, 840–5.
57 R. B. Weisman and S. M. Bachilo, *Nano Lett.*, 2003, **3**, 1235–1238.